Active elastic network: Cytoskeleton of the red blood cell

Nir S. Gov
Department of Chemical Physics, The Weizmann Institute of Science, P.O.B. 26, Rehovot, Israel 76100
(Received 25 September 2006; published 19 January 2007)

In red blood cells there is a cortical cytoskeleton; a two-dimensional elastic network of membrane-attached proteins. We describe, using a simple model, how the metabolic activity of the cell, through the consumption of ATP, controls the stiffness of this elastic network. The unusual mechanical property of active strain softening is described and compared to experimental data. As a by-product of this activity there is also an active contribution to the amplitude of membrane fluctuations. We model this membrane as a field of independent "curvature motors," and calculate the spectrum of active fluctuations. We find that the active cytoskeleton contributes to the amplitude of the membrane height fluctuations at intermediate wavelengths, as observed experimentally.

DOI: 10.1103/PhysRevE.75.011921 PACS number(s): 87.68.+z, 83.60.−a, 87.16.Ac, 87.17.−d

I. INTRODUCTION

The red-blood cell (RBC) has a cortical cytoskeleton, which is a two-dimensional network of cross-linked elastic proteins that are attached to and cover the entire inner surface of the cell membrane [1,2]. Such a cortical cytoskeleton gives the RBC the elasticity to survive repeated deformations [3]. The outstanding problem of understanding the physical properties of the RBC cytoskeleton has been to reconcile the measurements of the elasticity of the cell [3], the observed shapes of the RBC [4], and the measurements of the dynamic shape fluctuations of the membrane [5,6]. Our model attempts to reconcile these observation by showing that they follow naturally from our recently proposed mechanism of active remodeling of the RBC cytoskeleton [7]. In this paper we extend our recent theoretical modeling [7,8] and calculate several additional features of the active cytoskeleton. (i) We calculate the unique effect of strain-softening in this active network. The active dissociations of the network can account for the observed strain-softening of the RBC due to the dissociated filaments spending a longer time disconnected when the network is stretched. (ii) We then calculate the spectrum of active fluctuations, where we find that these contribute to the membrane height fluctuations at intermediate wavelengths, as observed experimentally.

The RBC cytoskeleton is a self-assembled network of flexible spectrin filaments that are end-attached to node complexes (Fig. 1). On average approximately six spectrin filaments attach to each actin node, mainly through the protein-4.1 [1,9], with a specific chemical affinity of order $\sim 7k_BT$. The flexible spectrin filaments are much longer ($\sim$200 nm) than the distance between the nodes that they connect [$R \sim 80-100$ nm, Fig. 1(a)], and can be treated as wormlike chains with an average end-to-end distance of [10]: $R_0 \sim 50-60$ nm. Each filament behaves (for small deformations) as a Hookean entropic spring, with a spring constant of [11]: $k \sim 20-40 k_BT/R^2 \sim 1 \times 10^{-5} \mathrm{J/m}^2$. At larger extensions a semiflexible chain behaves nonlinearly, and exhibits strain stiffening [12,13] and unfolding [14]. Note that the spectrin filaments are additionally connected to the membrane through the ankyrin-band-3 complex at random locations along the filaments, in between the actin-band-4.1 complexes at their ends [1]. It is the connections at the actin nodes that determine the overall connectivity of the network, and therefore dominate in controlling its elastic properties. We will therefore, also for simplicity of modeling, deal here with the active processes occurring at the filaments ends alone.

The elasticity of such a two-dimensional network, attached to the fluid bilayer, can be modeled as a static elastic network, with fixed connectivity [4,11,15]. Nevertheless, observations of membrane fluctuations [6] led to the speculation that ATP-induced phosphorylation of cytoskeleton proteins induces an overall softening. More recently, numerical simulations [4] recover the observed discocyte shape only

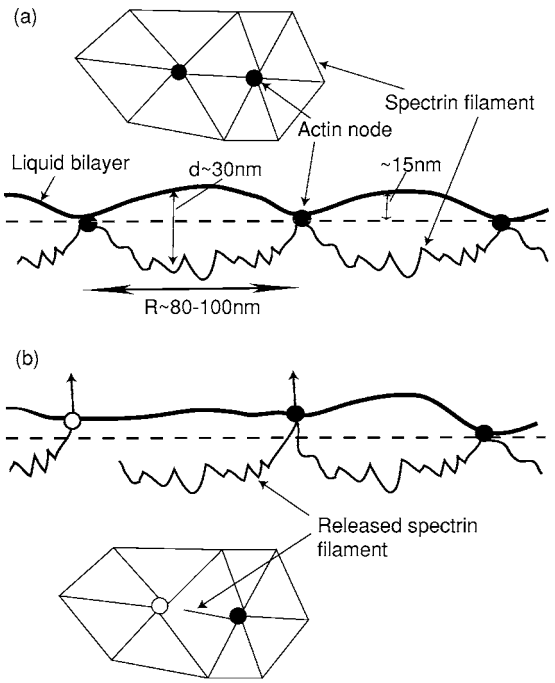

FIG. 1. A schematic illustration of our model of ATP-induced spectrin dissociation. The main parts of the figure show a side view of the RBC membrane, while the small parts show a schematic top view of the triangular cytoskeleton network. (a) The fully connected network, showing the balance between the stretched spectrin and curved bilayer. (b) The dissociated spectrin releases its stored tension. The phosphorylated node is indicated by the empty circle.

under the assumption that the cytoskeleton is able to relieve itself of all internal stresses. This stress-release process was attributed to an unspecified mechanism of cytoskeleton remodeling. While thermal dissociations in this network are highly unlikely, our main proposal [7] is that the cytoskeleton is an active structure that is constantly being remodeled by the consumption of ATP. Each ATP-induced phosphorylation of the protein-4.1 [16,17] causes a single spectrin filament to be dissociated from the actin node at one of its ends [Fig. 1(b)]. After each breaking event the proteins relax back to their initial states and spontaneously reattach due to their high specific chemical affinity.

II. ACTIVE STRAIN-SOFTENING

Let us first describe the elastic stiffness of the active elastic network (cytoskeleton). The transition rate from associated to dissociated spectrin is given by $k_{\mathrm{dis}}n_{\mathrm{ad}}$ where n_{ad} is the concentration of adsorbed ATP at the phosphorylation site (presumably at the protein-4.1) and k_{dis} is the dissociation rate of spectrin when ATP is attached (zero otherwise). The adsorption of ATP to the phosphorylation sites at the spectrin-actin junctions can be described by the equilibrium occupation probability [7], and from the experimental data on the ATP-induced fluctuations [18] indicates that it saturates ($n_{\mathrm{ad}}\sim 1$) at $n_{\mathrm{ATP}}> \sim 1.5$ mM, corresponding to normal RBC.

The reassociation rate k_{reas} depends on the relaxation processes; the time it takes the protein-4.1 to return to its dephosphorylated state and the time it takes the free spectrin end to "find" the node. The proportion of the time that the spectrin end is dissociated is given by

$$n_{\mathrm{dis}} = k_{\mathrm{dis}}n_{\mathrm{ad}}/(k_{\mathrm{dis}}n_{\mathrm{ad}} + k_{\mathrm{reas}}), \tag{1}$$

which is the proportion of dissociated spectrin ends n_{dis}. Considering that there are two dissociation sites per spectrin filament, the proportion of fully associated spectrin filaments is given by $n_{2a}=(1-n_{\mathrm{dis}})^2$, whereas the proportion of filaments that are cut at both ends is $n_{2\mathrm{dis}}\simeq n_{\mathrm{dis}}^2$. We expect the average shear modulus of the cytoskeleton network μ to be proportional to the fraction of fully associated filaments $\mu\propto n_{2a}$ [19]. This assumption means that we are restricted to strain rates that are smaller than the rate of dissociation-reassociation of cytoskeleton bonds [20].

Note that at the critical percolation limit p_c the shear modulus of a static network vanishes [19,21], while here the spectrin filaments continuously reconnect, so that in the limit of quasistatic shear we expect the linear relation between μ and n_{2a} to continue to hold even above p_c [7]. This situation is typical of "dynamic percolation" [20], whereby transport of mass and momentum occurs across the system due to its continuous renewals, even below the static percolation limit. On the other hand, finite size active networks at high strains and strain rates, may collapse ("melt") due to the ATP-induced dissociations, as was found in computer simulations [22].

The network is therefore softened by the effect of ATP-induced dissociations. Indeed, the shear modulus of an intact RBC (at physiological levels of ATP) is found to be approximately half that of the value for a cytoskeleton shell (no ATP) [23]. Using this result we fit for the intact RBC ($n_{\mathrm{ad}}\sim 1$) the value of the parameter $n_{\mathrm{dis}}\sim 1-1/\sqrt{2}\sim 0.3$, while both k_{dis} and k_{reas} are not known at present.

The full phosphorylation of protein-4.1 was recently [17] found to reduce the association of spectrin and actin, by a factor of ~ 2. As a consequence of this phosphorylation a reduction in the rigidity was observed [17], given by the average breaking-up time in shear flow. The break up occurs when the elastic deformation energy is greater than some minimum energy E_c needed to create detached vesicles. Assuming a simple spring elastic energy, the critical shear stretching will therefore be given by $\delta_c\propto\sqrt{E_c/\mu}$, and since the shear flow is kept constant, the time it takes to develop such an elongation will be $T_{\text{break-up}}\propto 1/\delta\propto\sqrt{\mu}$. We therefore predict that as the shear modulus gets reduced by a factor of ~ 2, the break-up time will be reduced by a factor of $\sim\sqrt{2}$, which is in excellent agreement with the observation [17]. These observations therefore support our model where the phosphorylation of protein-4.1 controls the spectrin-actin connectivity, which in turn determines the network stiffness.

So far we have described the linear elastic response of the RBC cytoskeleton in the limit of small and uniform deformations. A static network of flexible polymers, behaving as wormlike chains, is expected to show a strain-hardening behavior for pure stretching deformations that are larger than the linear regime [12,13]. Nevertheless, a significant strain softening was observed in highly aspirated RBCs [24,25], which indicates that either the network connectivity or the internal spectrin state (unfolding) is modified. The first of these possibilities results naturally from our model, which gives rise to a type of active-strain softening; When the network is stretched the time it takes the dissociated spectrin filaments to rebind is increased due to the longer path it has to cover. We assume here that the stretching of the filaments does not affect the rate of dissociations k_{dis}.

If we take that the reassociation time increases with the network elongation ($\lambda\equiv R/R_0$): $\tau_{\mathrm{reas}}=1/k_{\mathrm{reas}}\propto\lambda^{\alpha}$, the resulting network stiffness is given by

$$\mu(\lambda)\propto\mu_0(\lambda)\left(1+\frac{\tau_{\mathrm{reas}}}{\tau_{\mathrm{dis}}}\right)^{-2}=\mu_0(\lambda)(1+\lambda^{\alpha})^{-2}, \tag{2}$$

where $\tau_{\mathrm{dis}}=1/k_{\mathrm{dis}}$, and the strain hardening [13] is taken into account by the shear modulus of the fully connected network $\mu_0(\lambda)$ (inset of Fig. 2). The result is plotted in Fig. 2, where we fit the parameters such that the stiffness is normalized by that of the unstretched cell. We get a very good agreement with the data for stretched cells using $\alpha=16/7$ which is the expected dynamics for the longitudinal fluctuations of the free end of a semiflexible filament [26]. The excellent agreement at high extensions ($\lambda>2$) must be taken as somewhat fortuitous, since the strain stiffening $\mu_0(\lambda)$ was not calculated for such high extensions [13]. Note that the proposed dissociations between the cytoskeleton and the lipid bilayer [6], do not change the overall network stiffness and therefore do not explain the observed softening.

A similar effect of strain softening of the RBC network was observed in shear flow [27], where a lower overall

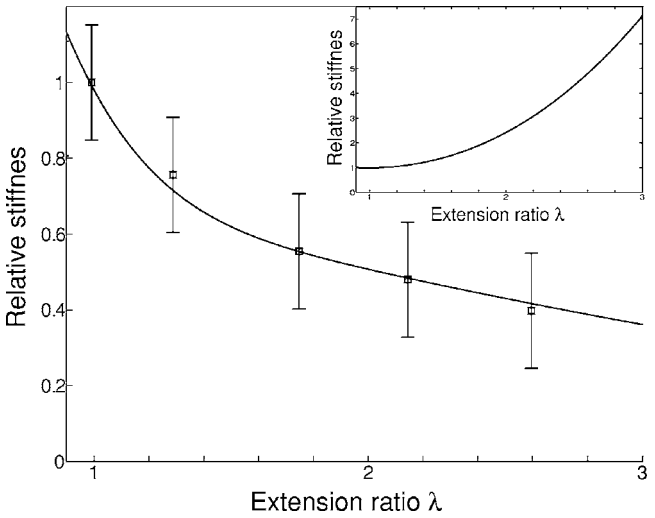

FIG. 2. Calculated strain softening of the RBC network shear elasticity μ as a function of the local elongation λ (solid line) from Eq. (2), compared to the experimental data (squares [24]). In the inset we plot the strain-stiffening of the fully connected network $\mu_0(\lambda)$, as calculated in Ref. [13].

spectrin-actin association was found as a function of increasing shear, in accordance with our model. In that work it was found that the spectrin tetramers break-up into dimers when the cell is sheared. This may be the result of the more frequent and longer spectrin-actin dissociations, since it is known that the tetramers break-up due to entropy when the filaments are not attached to the membrane [27]. The softening of RBC when they contain ATP should help them flow more easily through narrow capillaries. This was indeed observed as a correlation between the membrane height fluctuations and the transition time of the cells through porous filter [28]. More recently the cells were shown to behave in a fluidlike manner inside narrow capillaries [22]. Future experiments with ATP-depleted cells may probe the role of the active strain softening we describe above in the observed "fluidity" of the highly strained cells.

Note that we have analyzed above only quasistatic deformations. As the deformation-rate increases the fact that bonds are actually disconnected for a certain period of time will become more noticeable, and the network may breakdown for a large enough shear rate (and ATP-induced dissociation rate). Such catastrophic "tearing" of the active network under large shear rate is best studied by computer simulations [22].

III. SPECTRUM OF THE ACTIVE MEMBRANE FLUCTUATIONS

Next we describe the effects of the network activity on the spectrum of the shape fluctuations of the RBC [29]. We previously analyzed the active (ATP-induced) fluctuations of a single cytoskeleton element [7], and we wish here to go beyond the single unit cell and calculate the active fluctuation spectrum.

The main effect of the cytoskeleton on the thermal fluctuations of the membrane can be described phenomenologically [8] as an almost rigid shell that confines the amplitude of the bilayer fluctuations, such that $\langle h^2 \rangle \sim d \sim 30$ nm [Fig. 1(a)]. The coupling of a fluid bilayer to a solid (polymerized) membrane is more complex than this description, as we later showed in a more rigorous calculation [30], and is still an open problem [31,32]. Within the phenomenological model [8] the static fluctuation spectrum is given by

$$\langle h_q^2 \rangle = \frac{k_B T}{(\kappa q^4 + \sigma q^2 + \gamma)}, \tag{3}$$

where γ represents the harmonic confinement potential of the cytoskeleton and σ is significant only for wavelengths longer than those of a single cytoskeleton unit [8,33,30]. The data for normal RBC [29] was described reasonably well using the following elastic parameters [7]: $\gamma \sim 1-8\times 10^7$ J/m^4, $\sigma \sim 5-12\times 10^{-7}$ J/m^2, and $\kappa \sim 2-6\times 10^{-20}$ J. The confinement γ due to the cytoskeleton, limits the average amplitude of thermal fluctuations to $d^2 = k_B T/8\sqrt{\kappa\gamma} \sim (20-30)^2$ nm^2 [8]. Note that the confinement by the cytoskeleton also affects (slows down) the frequency of the membrane bending modes [8,34,35]. The frequency of the bending modes of a free membrane is given by $\omega_m(q) = (\kappa q^4 + \sigma q^2)\Lambda(q)$, where $\Lambda_{\text{free}}(q) = 1/4\eta q$ is the Oseen hydrodynamic interaction and η is the viscosity of the surrounding fluid. In the confined geometry we showed that the Oseen kernel is modified [34]; $\Lambda_{\text{con}}(q) = \Lambda_{\text{free}}(q)\exp(-2qd) \quad [-1+\exp(2qd)-2qd-2(qd)^2]$, such that in the limit of $q \to 0$ we now get

$$\Lambda_{\text{con}}(q) \to d^3 q^2/3\eta, \; \omega_{m,0} \to \gamma d^3 q^2/3\eta. \tag{4}$$

Within this model the effect of ATP on the thermal component of the membrane fluctuations is through the changes in the elastic parameters σ and γ. Both these parameters are linearly proportional to the average shear modulus μ [34], and so are expected to change by up to a factor of ~ 2 when ATP is depleted and the cell shape changes to echinocyte. The overall shape of the fluctuation spectrum should not change significantly, beyond the rescaling of the amplitude. The active component of the membrane fluctuations cannot be described purely to arise from a change in the elastic parameters, since it was shown to depend on the fluid viscosity [36], unlike thermal fluctuations. Below we shall describe the spectrum of this active contribution using a quantitative model, instead of the *adhoc* effective temperature parameter used previously [8].

The enhanced amplitude of the membrane fluctuations of the normal cell is due in our model to the release of stored tension in the spectrin filament and bilayer in each dissociation event. The ATP can induce in this manner membrane height fluctuations, through repeated "pinching" of the membrane by the cytoskeleton (Fig. 1). Previously we considered the active fluctuations of a single unit cell [7], while here we describe a uniform field of such active membrane units [37]. We assume that the units are uncorrelated with each other, and their on-site temporal correlations are given by a simple shot-noise behavior, characterized by a single timescale τ [37]. This timescale represents the duration of force production, of magnitude F. Since the bilayer is fluid the cytoskeleton-induced forces become uniformly distributed.

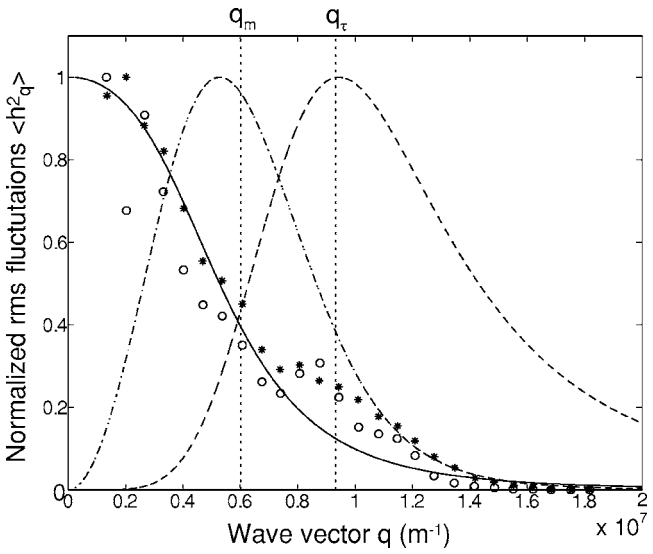

FIG. 3. Static fluctuation spectrum of the membrane of a normal RBC membrane $\langle h_q^2 \rangle$: stars and circles [29]. The solid line is the thermal component using Eq. (3), dashed and dash-dot lines are the active component of the curvature motor and direct force, respectively, using Eq. (5). A value of τ=50 ms was used in these calculations. Vertical dotted lines give q_m (left) and q_τ (right), respectively.

We shall consider two types of possible modes of ATP-induced forces at the membrane; a direct force and a "curvature motor," that introduces a local, fluctuating, curvature in the bilayer [37]. The curvature force produced by each active cytoskeleton unit couples to the curvature $\nabla^2 h$ [37], through an active spontaneous curvature $H=1/r$ induced in the membrane by the "pinching" action of the cytoskeleton (Fig. 1). We estimated the force balance between the spectrin compression and the membrane bending [7], and found that $r \sim R \sim 100$ nm (Fig. 1).

The amplitude of active fluctuations for such a model [37], is given by

$$\langle |h(q)|^2 \rangle_{\text{active},c} = [\Lambda_{\text{con}}(q) F (qr)^2]^2 \frac{n}{2\omega_m(q)[\omega_m(q) + 1/\tau]},$$

$$\langle |h(q)|^2 \rangle_{\text{active},d} = [\Lambda_{\text{con}}(q) F]^2 \frac{n}{2\omega_m(q)[\omega_m(q) + 1/\tau]} \quad (5)$$

for the curvature and direct forces, respectively, and where $\omega_m(q)$ is the temporal response of the confined bilayer [Eq. (4)], $n \sim n_{\text{dis}}/R^2$ is the areal density of active membrane units, where the probability of the unit to be in its "on" state is given by the spectrin dissociation probability n_{dis}, and $F \sim 0.2$ pN is the force of the cytoskeleton unit [7]. Since n_{dis} depends on the concentration of ATP, so does the amplitude of the active fluctuations, as is observed experimentally [18].

Since the active and thermal fluctuations are incoherent, we have $\langle |h(q)|^2 \rangle_{\text{total}} = \langle |h(q)|^2 \rangle_{\text{active}} + \langle |h(q)|^2 \rangle_{\text{thermal}}$, and we plot both contributions in Fig. 3. Note that in the limit of $q \to 0$ the active contribution vanishes, while it is most dominant at intermediate q values. The peak contribution for the curvature motor occurs roughly at q_τ defined by $\omega_m(q) = 1/\tau$, while the maximum of the direct-force occurs roughly at $q_m \sim (\gamma/\kappa)^{1/4}$ (Fig. 3). The observed active contribution to the membrane fluctuations is of the order of the thermal component [7,18], which using the pervious values of the parameters gives us an estimate of the time scale $\tau \sim 10-100$ msec.

We expect from our model, using Eqs. (5), that when the RBC is depleted of ATP its rms membrane fluctuation amplitude at $q \to 0$ should be diminished by up to a factor of 2 due to the increase in the cytoskeleton elastic stiffness and the subsequent reduction in the thermal fluctuations. The active contribution should appear as a "surplus" amplitude at intermediate q values, which may correspond to the observed "jump" in the measured data [29] (Fig. 3), which was previously described in terms of passive effects of the cytoskeleton [8,31,33]. We show here that this feature may be due to the active fluctuations, and should therefore be smaller when the ATP is depleted. From Fig. 3 it seems that the experimental data corresponds to our calculation for the curvature-motor spectrum (Fig. 1). Detailed comparison to high resolution experimental spectrum [38] may allow us to determine which mode of active membrane forces is appropriate for the RBC.

Our model predicts that the mean-square amplitude of the active fluctuations [Eqs. (5)–(7) below] are inversely proportional to the viscosity of the surrounding fluid η. This behavior has been measured by changing the viscosity using various chemical agents [5,36]. Any specific chemical effect is therefore unlikely, and these experiment give a clear sign of active processes, since the amplitude of thermal fluctuations [Eq. (3)] is independent on any dynamic quantities such as viscosity.

For the sake of completeness we also give the active fluctuations if the hydrodynamic confinement does not affect this component. This may be motivated by the fact that the active units are themselves forming the confining cytoskeleton and their active dissociation may therefore be less affected. In this case we replace in Eq. (5) the hydrodynamic interaction function by $\Lambda_{\text{free}}(q)$. The results are very different; In the limit $q \to 0$ the amplitude of height fluctuations for the curvature-motors approaches a constant, given by

$$\langle |h(q)|^2 \rangle_{\text{active},c} \to \frac{3F^2 n \tau r^4}{32 \eta \gamma d^3}. \quad (6)$$

If we wish this active contribution to be of the order of the thermal one, we fit $\tau \sim 0.5-1$ msec. By comparing Eqs. (3) and (6) in the limit of $q \to 0$, we can define an "effective temperature" of the active fluctuations [7,37]: $\langle |h(0)|^2 \rangle_{\text{thermal}} = k_B T/\gamma \Rightarrow k_B T_{\text{eff},c} = (3F^2 n \tau r^4)/(32 \eta d^3)$, which gives the observed $T_{\text{eff},c}/T \sim 1.5$ [8,18] using $\tau \sim 1$ msec. For the direct-force case the amplitude of active fluctuations now diverges at $q \to 0$. The divergence in this limit coincidentally resembles that of a free membrane [Eq. (3) for $\sigma, \gamma = 0$], which we can then use to define another effective temperature

$$\langle |h(q)|^2 \rangle_{\text{active},d} = _{q\to 0} \frac{k_B T_{\text{eff},d}}{\kappa q^4}$$

$$\Rightarrow k_B T_{\text{eff},d} = \frac{3\kappa F^2 n \tau}{32 \eta \gamma d^3} \quad (7)$$

which gives a numerical value close to that of $T_{\text{eff},c}$ for the curvature motor, since $\kappa/\gamma \sim r^4$ [8].

IV. CONCLUSION

We introduced a concept of a two-dimensional elastic network that is actively being broken and reassembled, as occurs in the RBC. Such active networks present an interesting physical system, which goes beyond the domain of static random networks. We show that the elastic properties and the dynamic fluctuations of these networks are very different, sometimes behaving in an opposite way, from their in-active counterparts. Note that since the RBC is a complex system there are other cellular mechanism that influence the elastic strength and membrane fluctuations, which we have not considered here. Rather we wish here to emphasize the consequences of the proposed activity of the cytoskeleton, for the RBC case and in general.

Similar cortical cytoskeleton to that of the RBC exists on the membranes of most mammalian cells and on the membranes of internal organelles such as Golgi [39]. These cortical networks are not always composed of spectrin, but of a host of similar intermediate filaments [40]. We therefore expect all of these networks to be active as in the RBC case. For example, non-RBC cells [41] also show marked stiffening, contraction and formation of spicules under ATP depletion or Ca^{2+} loading, as was found for the RBC [7]. Understanding the inner workings of the active cortical cytoskeleton may have implications for combating various diseases, such as malaria in the case of the RBC [7,42]. Furthermore, we expect that the activity of the cortical cytoskeleton will contribute to the observed membrane height fluctuations in many cell types [43], similar to what we calculate here for the RBC.

Active networks may also be a useful engineering tool when making biomimetic structures for drug delivery, biomimetic devices, and sensors. To make these scaffolds active an energy source is needed of course, which inside the body may be in the form of ATP. Future studies using better theoretical modeling, detailed simulations [22] and experiments will allow a better understanding of the fascinating physical properties of these active (living) networks [25,44].

ACKNOWLEDGMENTS

I thank Sam Safran, Thorsten Auth, Itay Rousso, and Arkady Bitler for useful discussions. I thank the ISF grant, the EU SoftComp NoE grant, and the Robert Rees Fund for Applied Research, for their support.

[1] V. Bennett, Biochim. Biophys. Acta **988**, 107 (1989).
[2] S. Tsukita, S. TITA, and H. Ishikawa, J. Cell Biol. **85**, 567 (1980).
[3] D. E. Discher and P. Carl, Cell. Mol. Biol. Lett. **6**, 593 (2001).
[4] J. Li, M. Dao, C. T. Lim, and S. Suresh, Biophys. J. **88**, 3707 (2005); M. Dao, J. Li, and S. Suresh, Mater. Sci. Eng., C **26**, 1232 (2006).
[5] K. Fricke and E. Sackmann, Biochim. Biophys. Acta **803**, 145 (1984).
[6] E. Sackmann, FEBS Lett. **346**, 3 (1994).
[7] N. Gov and S. Safran, Biophys. J. **88**, 1859 (2005).
[8] N. Gov, A. G. Zilman, and S. Safran, Phys. Rev. Lett. **90**, 228101 (2003).
[9] W. Nunomura and Y. Takakuwa, Front. Biosci. **11**, 1522 (2006).
[10] K. Svoboda, C. F. Schmidt, D. Branton, and S. M. Blockt, Biophys. J. **63**, 784 (1992).
[11] S. K. Boey, D. H. Boal, and D. E. Discher, Biophys. J. **75**, 1573 (1998).
[12] P. R. Onck, T. Koeman, T. van Dillen, and E. van der Giessen, Phys. Rev. Lett. **95**, 178102 (2005); C. Storm, J. J. Pastore, F. C. MacKintosh, T. C. Lubensky, and P. A. Janmey, Nature (London) **435**, 191 (2005).
[13] J. C. Hansen, R. Skalak, S. Chien, and A. Hoger, Biophys. J. **70**, 146 (1996).
[14] R. Law, P. Carl, S. Harper, P. Dalhaimer, D. W. Speicher, and D. E. Discher, Biophys. J. **84**, 533 (2003).
[15] F. Tessier, D. H. Boal, and D. E. Discher, Phys. Rev. E **67**, 011903 (2003).
[16] M. Nakao, Curr. Opin. Hematol. **9**, 127 (2002); E. Ling, Y. N. Danilov, and C. M. Cohen, J. Biol. Chem. **263**, 2209 (1988); K. N. Pestonjamasp and N. G. Mehta, Exp. Cell Res. **219**, 74 (1995).
[17] S. Manno, Y. Takakuwa, and N. Mohandas, J. Biol. Chem. **280**, 7581 (2005).
[18] S. Tuvia, S. Levin, A. Bitler, and R. Korenstein, J. Cell Biol. **141**, 1551 (1998).
[19] J. C. Hansen, R. Skalak, S. Chien, and A. Roger, Biophys. J. **72**, 2369 (1997).
[20] S. D. Druger, A. Nitzan, and M. A. Ratner, J. Chem. Phys. **79**, 3133 (1983).
[21] D. Vernon, M. Pilschke, and B. Joós, Phys. Rev. E **64**, 031505 (2001).
[22] J. Li, M. Dao, and S. Suresh (unpublished).
[23] G. Lenormand, S. Hénon, A. Richert, J. Siméon, and F. Gallet, Biorheology **40**, 247 (2003).
[24] J. C-M. Lee and D. E. Discher, Biophys. J. **81**, 3178 (2001).
[25] J. C-M. Lee, D. T. Wong, and D. E. Discher, Biophys. J. **77**, 853 (1999); D. E. Discher and N. Mohandas, *ibid.* **71**, 1680 (1996); D. E. Discher, N. Mohandas, and E. A. Evans., Science **266**, 1032 (1994).
[26] R. Everaers, F. Jülicher, A. Ajdari, and A. C. Maggs, Phys. Rev. Lett. **82**, 3717 (1999).
[27] X. An, M. C. Lecomte, J. A. Chasis, N. Mohandas, and W.

Gratzer, J. Biol. Chem. **277**, 31796 (2002).
[28] S. Tuvia, S. Levin, and R. Korenstein, FEBS Lett. **304**, 32 (1992).
[29] A. Zilker, H. Engelhardt, and E. Sackmann, J. Phys. (Paris) **48**, 2139 (1987).
[30] N. Gov and S. A. Safran, Phys. Rev. E **69**, 011101 (2004).
[31] C. Dubus and J.-B. Fournier, Europhys. Lett. **75**, 181 (2006).
[32] S. B. Rochal and V. L. Lorman, Phys. Rev. Lett. **96**, 248102 (2006).
[33] J. B. Fournier, D. Lacoste, and E. Raphael, Phys. Rev. Lett. **92**, 018102 (2004).
[34] N. Gov, A. G. Zilman, and S. Safran, Phys. Rev. E **70**, 011104 (2004).
[35] Y. Kaizuka and J. T. Groves, Phys. Rev. Lett. **96**, 118101 (2006).
[36] S. Tuvia, A. Almagor, A. Bitler, S. Levin, R. Korenstein, and S. Yedgar, Proc. Natl. Acad. Sci. U.S.A. **94**, 5045 (1997).
[37] N. Gov, Phys. Rev. Lett. **93**, 268104 (2004).
[38] G. Popescu, K. Badizadegan, R. R. Dasari, and M. S. Field, J. Biomed. Opt. **11**, 040503 (2006); G. Popescu *et al.*, Phys. Rev. Lett. **97**, 218101 (2006).
[39] M. C. Stankewich *et al.*, Proc. Natl. Acad. Sci. U.S.A. **95**, 14158 (1998).
[40] A. Bretscher, Annu. Rev. Cell Biol. **7**, 337 (1991).
[41] M. Street, S. J. Marsh, P. R. Stabach, J. S. Morrow, D. A. Brown, and N. J. Buckley, J. Cell. Sci. **119**, 1528 (2006).
[42] S. Suresh, J. Spatz, J. P. Mills, A. Micoulet, M. Dao, C. T. Lim, M. Beil, and T. Seufferlein, Acta Biomater. **1**, 15 (2005).
[43] A. Zidovska and E. Sackmann, Phys. Rev. Lett. **96**, 048103 (2006).
[44] H. W. G. Lim, M. Wortis, and R. Mukhopadhyay, Proc. Natl. Acad. Sci. U.S.A. **99**, 16766 (2002).